Hindawi
Shock and Vibration
Volume 2019, Article ID 8652894, 19 pages
https://doi.org/10.1155/2019/8652894

Research Article

Movement Law and Discriminant Method of Key Strata Breakage Based on Microseismic Monitoring

Yang Li,[1,2] **Tianhong Yang**,[3] **Weidong Song**,[1,2] **and Ling Yu**[4]

[1]*Key Laboratory of Ministry of Education for Efficient Mining and Safety of Metal Mines, University of Science and Technology Beijing, Beijing 100083, China*
[2]*School of Civil and Resource Engineering, University of Science and Technology Beijing, Beijing 100083, China*
[3]*Center of Rock Instability and Seismicity Research, School of Resources & Civil Engineering, Northeastern University, Shenyang, Liaoning 110819, China*
[4]*Institute of Opencast Mining Safety, CCTEG Shenyang Research Institute, Fushun, Liaoning 113122, China*

Correspondence should be addressed to Yang Li; leon.42@163.com

Received 27 March 2019; Revised 12 July 2019; Accepted 24 July 2019; Published 26 August 2019

Academic Editor: Radoslaw Zimroz

Because of the unique natural geography, geological structure, and ecological environment, there are serious geological disasters and environmental damage caused by the high-intensity mining in Western China. It seriously restricts the development of coal resources and the protection of ecological environment. In order to fully capture the law of key stratum breakage with high-intensity mining, the IMS microseismic system was introduced into Xiaojihan coal mine which is a typical high-intensity mining mine in Western China, and the whole process dynamic monitoring was carried out. The process of key stratum breakage was analysed by MS data, which were in agreement with the pressure analysis results of the hydraulic support of the working face. The results showed that there were the obvious forewarning characteristics in microseismic event number, energy release, energy index, Schmidt number, coefficient of seismic response, and b value when the key stratum was breaking. Then, a method to discriminate the breakage of key stratum was proposed by using the forewarning characteristics, which could provide the guidance for prevention and control of geological hazards in the working face with high-intensity mining.

1. Introduction

Presently in China, the exploitation of coal resource has been transferred to Western China [1], which possesses the unique natural geography, geological structure, and ecological environment. Consequently, the high-intensity mining in Western China has caused serious geological disasters and environmental damage [2]. It seriously restricts the coal exploitation and the ecological protection, which has drawn much attention from the Chinese government [3]. High-intensity coal mines such as Daliuta Coal Mine, Ciyaowan Coal Mine [4], and Longde Coal Mine [5] have suffered from geological disasters such as roof collapse and water and sand inrush, resulting in many deaths and huge economic losses. In order to achieve safe production, it is very urgent to carry out research on rock mass failures and strata movement under high-intensity mining conditions.

Since key stratum (KS) is a rock stratum that completely or partially controls rock mass activity, KS movement plays a significant role for the stability of the whole strata. Since Qian et al. [6] put forward KS theory, many scholars have studied it. Through model experiment, field measurement, and numerical simulation, Miao et al. [7, 8] studied the breakage and collapse feature of KS around coal face and its influence on rock pressure in fully-mechanized coal face.

Microseismic (MS) monitoring is a technical method to monitor the stability of engineering rock mass by using elastic wave generated by rock deformation and failure. By the middle of last century, MS monitoring has been widely used in Poland, South Africa, the United States, Canada, and other major mining countries [9–12]. Compared with foreign countries, MS monitoring in China started late. But in the recent years, it has been developed rapidly, with a lot of research work being carried out in the fields of MS theory

research, rock burst prediction and early warning, mine water inrush risk prediction, and slope stability analysis. And many valuable research results have been obtained [13–16]. In addition, some MS monitoring of KS has been carried out. The shock bump caused by KS motion is studied by MS monitoring technology [17]. The fracture mechanism of overlying rock mass and its influence are studied by combining theoretical analysis with MS monitoring [18–22]. Jiang et al. [23, 24] analysed the MS activity characteristics of high-position hard thick KS and high-located main KS. The research of these scholars has laid a good foundation for the study of KS with the combination of strata movement theory and MS monitoring.

At present, KS breakage is mainly studied by theoretical analysis and numerical simulation, which makes it difficult to reveal the true form of the KS breakage in mine. MS monitoring is an effective means of monitoring. It can not only reflect the specific situation of KS breakage but also provide the site basis for the stability and breakage discrimination of KS through the relevant study of MS parameters. In this paper, we introduce the MS monitoring system into Xiaojihan coal mine, which is a typical high-intensity mining mine in Western China. Through real-time monitoring, the relationship between KS fracture and MS event characteristics is studied, and a KS fracture discrimination method based on MS parameters is proposed. This provides both a basis for the study of roof stability and disaster prevention under the condition of high-intensity mining and a reference for MS monitoring of high-intensity mining face.

2. Geomining Conditions of Xiaojihan Coal Mine

Xiaojihan coal mine is the first modern coal mine produced by 10 million tons in Yuheng mining area of Jurassic coalfield in North Shaanxi Province. The mine is located in Yuyang District, Yulin City, Shaanxi Province, 12 km west of Yulin City. The mining area covers an area of 25.175 km^2, with 3.17 billion tons of geological reserves and 1.89 billion tons of recoverable reserves. There are nine seams in the mineable coal seams, of which 2# and 4^{-2}# seams are the main ones. The geological structure of the mine is simple, with the horizontal coal seam and the dip angle of less than 1°. At the same time, Xiaojihan coal mine belongs to low gaseous mine. The mine adopts inclined shaft development and belt mining, and its designed production capacity is 10 Mt/a.

Fully mechanized working face 11203 is the first mining face of Xiaojihan coal mine, located in panel 11 of 2^{-2}# coal seam. The floor elevation of coal seam in working face 11203 is 826 to 890 m, and the ground elevation is 1208 to 1225 m. The advance length of working face before retracement is 2651.2 m, and the face width is 240 m. The dip angle of coal seam is 0 to 1°, with the average of 0.7°. In working face 11203, inclined longwall fully mechanized mining method and all-collapsing method of treatment are adopted. There are two production shifts and one maintenance shift every day. The maintenance shift needs to ensure the coal cutting 2 knives, and the rest of the time for equipment maintenance. Two production shifts are mining all the time, and each shift cut coal 5 knives. Every knife cutting depth of the coal mining machine is 865 mm. Therefore, mining speed of working face 11023 can reach 8 to 10 m/d, which is a typical high-intensity mining working face.

3. Establishment of a MS Monitoring System

According to the characteristics of working face mining, it was appropriate to select the speed sensor with natural frequency of 14 Hz, monitoring range of 9 Hz~2000 Hz, and response range of hundreds of meters. The sensor layout had been optimized by considering the spatial characteristics of rock mass fracture and the convenience of MS sensor installation. For eight channels data acquisition, it was reasonable to adopt five uniaxial speed sensors and one triaxial speed sensor. The six sensors were installed in the auxiliary transport roadway of working face 11203 (Figure 1). The first sensor distance from working face open-off cut is 100 m, and distance between each sensor is 40 m. Among them, the fourth sensor is triaxial speed sensor. The sensor layout is shown in Figure 2. The error of the source location was obtained by comparing the measuring coordinates and the coordinates of MS analysis (Table 1). The detection of blasting location shows that the measurement results are close to the analysis results and the source location accuracy of the system is reasonable. The fundamental principle and technical parameters of the MS monitoring technique are detailed in the author's previous research [25], and the MS monitoring data in this paper are based on the existing MS monitoring system.

4. MS Event Distribution of the KS Breakage

4.1. Discrimination of the KS of Working Face 11203

4.1.1. Law of the KS Breakage. Qian et al. [6] first proposed the KS theory of overlying strata activity in stope. Because of the different stratification characteristics of coal and rock mass, the roles of each stratum in rock mass activities are also different. Some hard and thick strata control the movement of rock mass, which can also be called supporting body or skeleton. Some weak and thin strata play a load role in rock mass activities, and most of their weight is borne by hard and thick rocks. Therefore, the strata that mainly control the activity of rock mass are called KS. And, the definition of KS is as follows: when there are many strata in the overburden strata of the stope, the strata controlling all or part of the rock mass activity are called KS. The former is called the main KS of strata activity, and the latter is called the inferior KS [26].

The strata group moves from bottom to top, and the dynamic process of strata movement is controlled by KS breakage. Assuming that the overlying strata have three KS from bottom to top, the strata movement is shown in Figure 3. When inferior KS 1 is broken, the rock groups controlled by inferior KS 1 are broken at the same time, and bed separation occurs below lower KS 2 (see Figure 3(a)).

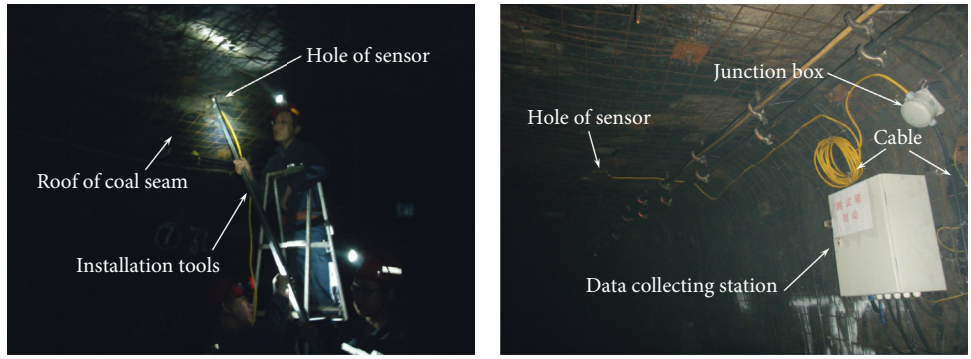

(a) (b)

Figure 1: Field installation of the IMS monitoring system: (a) IMS sensor; (b) IMS system.

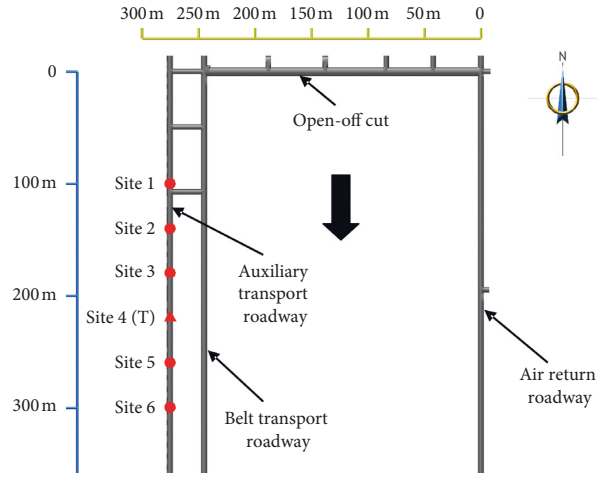

Figure 2: Specific arrangement of MS monitoring.

Table 1: Locating results of the blasting events.

Number	Blasting position (m)		Event location (m)		Error (m)
1	X	4261320.940	X	4261318	6
	Y	37368561.987	Y	37368567	
	Z	865.574	Z	868	
2	X	4261287.486	X	4261293	8
	Y	37368550.793	Y	37368546	
	Z	862.182	Z	866	

When the inferior KS 2 is broken, the rock groups controlled by the inferior KS 2 are broken. Bed separation occurs below the main KS (Figure 3(b)). Once the main KS breaks down, all strata overlying the surface will break down and sink simultaneously (Figure 3(c)) [26].

4.1.2. Discriminant Method KS. According to the definition of the KS and its deformation characteristics, when there are n rock strata synchronously deformed, the lowest rock stratum is the KS. It can be seen from the supporting characteristics of the KS:

$$q_1 > q_i, \quad i = 2, 3, \ldots, n. \tag{1}$$

The deformation of rock stratum $n+1$ is less than that of rock stratum n; the rock strata above the rock stratum $n+1$ no longer need its lower rock to bear any load it bears. There must be [26]

$$q_1|_{n+1} > q_1|_n, \tag{2}$$

where

$$q_1|_{n+1} = \frac{E_1 h_1^3 \left(\sum_{i=1}^{n} \gamma_i h_i + q_{n+1}\right)}{\sum_{i=1}^{n+1} E_1 h_1^3}. \tag{3}$$

In equation (3), when $n+1 = m$, $q_{n+1} = \gamma_m h_m + q$; when $n+1 < m$, q_{n+1} can be obtained by using the method of solving q_1. When the rock stratum $n+1$ can control the rock stratum m,

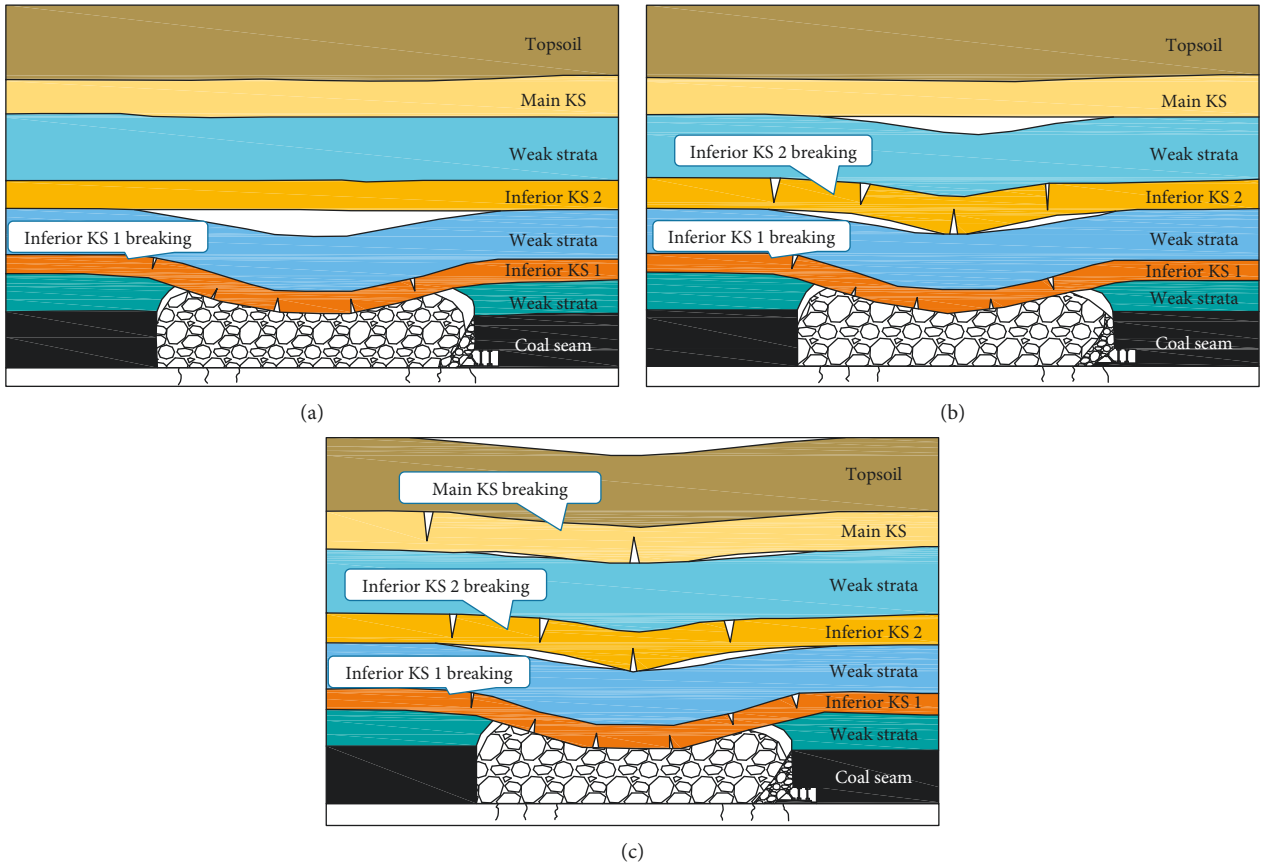

Figure 3: Dynamic process of the overlying rock movement. The breakage of inferior (a) KS 1, (b) KS 2, and (c) main KS.

$$q_{n+1}\big|_{m-n} = \frac{E_{n+1}h_{n+1}^3\left(\sum_{i=n+1}^{m}\gamma_i h_i + q\right)}{\sum_{i=n+1}^{m}E_{n+1}h_i^3}. \tag{4}$$

When the rock stratum $n+1$ cannot control the rock stratum m, q_{n+1} could be still obtained by using the form of q_1 in equation (3) to calculate the load of the rock stratum $n+1$ until the solution can control the rock stratum m.

Equation (2) is the comparative form of the load, which is the stiffness (deformation) criterion of the KS. It means that the deflection of the rock stratum $n+1$ is less than the deflection of the lower rock strata. When $n+1<m$, the rock stratum $n+1$ is not the boundary layer. Therefore, it is necessary to understand the load and strength conditions of rock stratum $n+1$. In this case, the rock stratum $n+1$ may be KS, but it must also satisfy the strength condition. When the rock stratum $n+1$ is KS, its breaking interval is l_{n+1}, the breaking interval of the first rock stratum is l_1, and the strength criterion of the KS is as follows [26]:

$$l_{n+1} > l_1. \tag{5}$$

Here, the first rock is the inferior KS. When l_{n+1} cannot meet the equation (5), all the rock strata controlled by the rock stratum $n+1$ should be acted as load to the rock stratum n to calculate the deformation and breaking interval of the rock stratum n.

Under the premise of equations (2) and (5), it is possible to distinguish the thickness and number of the rock strata that the KS 1 can control. When $n=m$, the KS 1 is the main KS; When $n<m$, the KS 1 is the inferior KS.

In the movement process of the overlying rock mass from the bottom to the top in the stope, the rock mass movements are not all passed up stratum by stratum, and sometimes there are two or more than two rock strata moving synchronously (including simultaneous breakage without interstratum dislocation). The rock strata with this synchronous movement are called composite rock stratum. If the composite rock stratum is KS, it is called composite KS. The composite effects of obvious stiffness and strength increase are produced between two adjacent hard rock strata, and the lithology and geometric characteristics of the adjacent hard rock strata are defined as follows: (1) the lithology of the two hard rock strata are basically the same, and the weak rock strata between them are distinctly different from them. (2) Thickness of the hard and the weak rock strata are not different in magnitude [26].

4.1.3. Discriminant Result of KS. According to the discriminant method of KS in Section 4.1.2, the discriminant result of the KS in the working face 11203 is shown in Table 2. It can be seen that there are four inferior KS and a main KS in the working face 11203, among which the inferior KS 3 and the main KS are both combined with two hard rock strata. According to the location and distribution characteristics of MS events (Figure 4), the fracture of rock should be within

Table 2: Identification of the KS in working face 11203.

Number	Thickness (m)	Depth (m)	Name	Hard rock	KS
38	7.00	7.00	Silty-fine sand		
37	28.72	35.72	Fine-silty sand		
36	13.69	49.41	Sandy loam		
35	**15.24**	**64.65**	Medium-grained feldspar sandstone	Yes	Main KS (composite KS, combined two hard rock strata)
34	5.50	70.15	Mudstone		
33	**26.67**	**96.82**	Fine feldspar sandstone	Yes	
32	6.87	103.69	Sandstone		
31	14.87	118.56	Siltstone		
30	8.49	127.05	Silty mudstone		
29	7.89	134.94	Fine feldspar sandstone		
28	6.43	141.37	Mudstone		
27	**29.67**	**171.04**	Fine feldspar sandstone	Yes	Inferior KS 4
26	9.54	180.58	Siltstone		
25	10.87	191.45	Mudstone		
24	6.77	198.22	Fine feldspar sandstone		
23	3.99	202.21	Mudstone		
22	3.33	205.54	Fine feldspar sandstone		
21	3.30	208.84	Mudstone		
20	6.89	215.73	Fine feldspar sandstone		
19	7.29	223.02	Silty mudstone		
18	3.44	226.46	Mudstone		
17	8.90	235.36	Silty mudstone		
16	**9.49**	**244.85**	Fine feldspar sandstone	Yes	Inferior KS 3 (composite KS, combined two hard rock strata)
15	6.68	251.53	Silty mudstone		
14	9.39	260.92	Pelitic siltstone		
13	**10.05**	**270.97**	Fine feldspar sandstone	Yes	
12	5.30	276.27	Mudstone		
11	7.63	283.90	Silty mudstone		
10	11.29	295.19	Mudstone		
9	**11.53**	**306.72**	Medium-grained feldspar sandstone	Yes	Inferior KS 2
8	11.80	318.52	Silty mudstone		
7	6.20	324.72	Coarse feldspar sandstone		
6	3.99	328.71	Silty mudstone		
5	1.64	330.35	Fine feldspar sandstone		
4	7.17	337.52	Silty mudstone		
3	**7.51**	**345.03**	Fine feldspar sandstone	Yes	Inferior KS 1
2	3.99	349.02	Silty mudstone		
1	2.95	351.97	Coal stratum 2#		

80 m above the coal seam. Therefore, the fracture or breakage of KS is inferior KS 1 and KS 2. This means that the pressure behavior of the working face is affected by these two inferior KS. The following focuses on the relationship between the MS event activity and the breakage of the inferior KS 1 and 2.

4.2. MS Event Evolution of the Breakage of KS

4.2.1. Location Results of MS Event. The main roof is an inferior KS influencing the mine pressure behavior [27], as shown in Table 2. The breakage of main roof is the breakage of the inferior KS. This paper chooses the MS data from Aug 20, 2013, to Sep 11th, 2013, to study the evolution process of KS breakage. The location of MS event from Aug 31 to Sep 10 is shown in Figure 5.

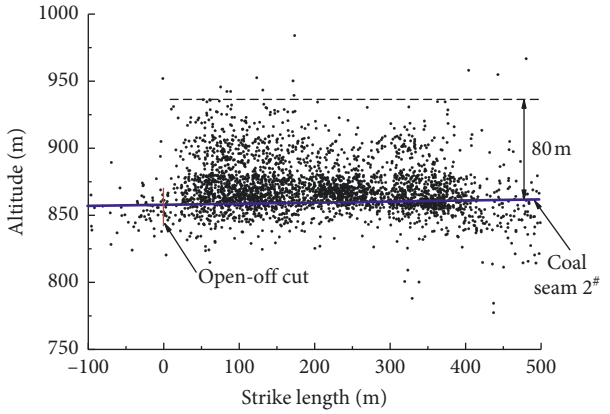

Figure 4: Location of microseismic events along the strike direction.

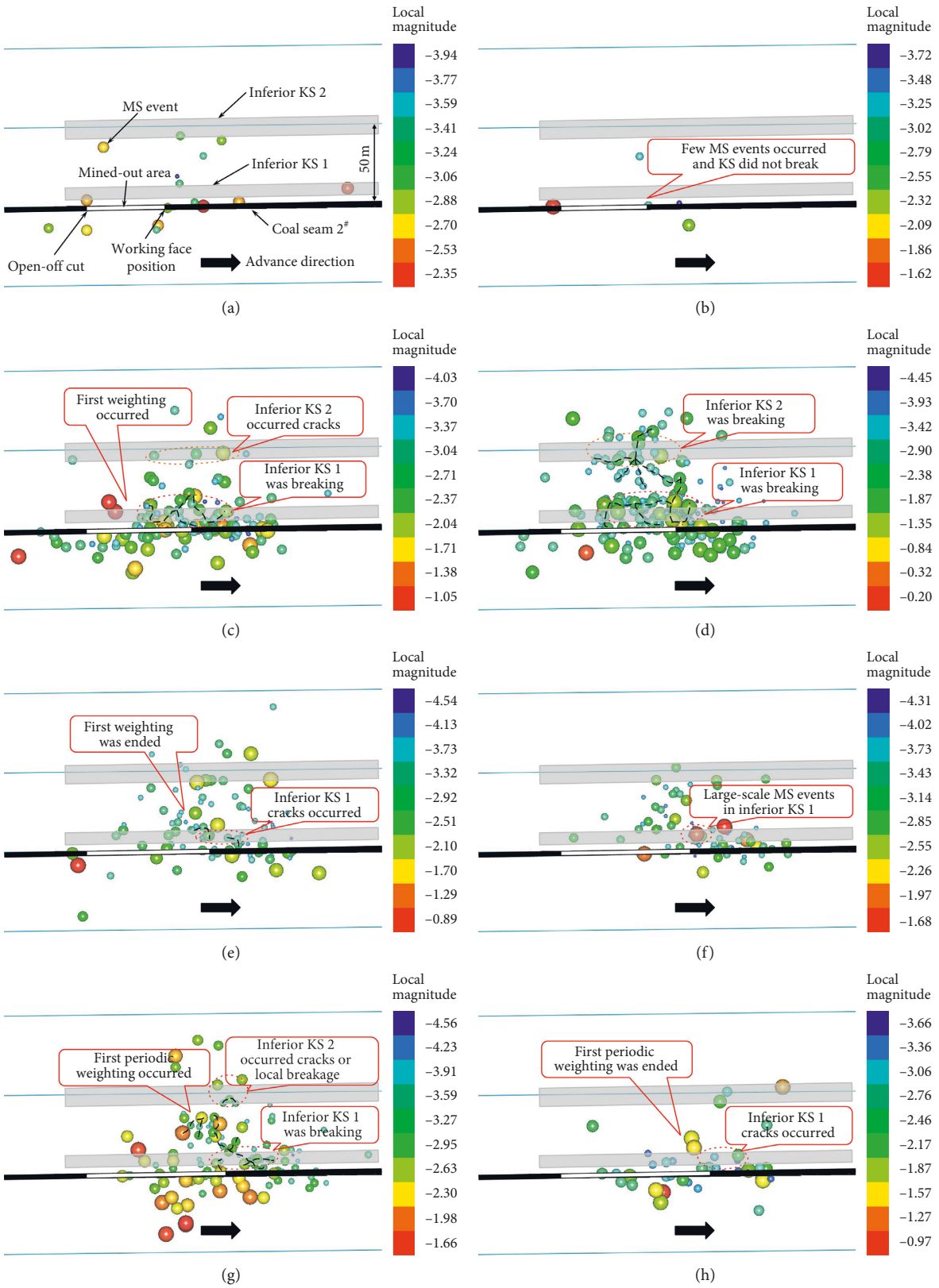

Figure 5: Continued.

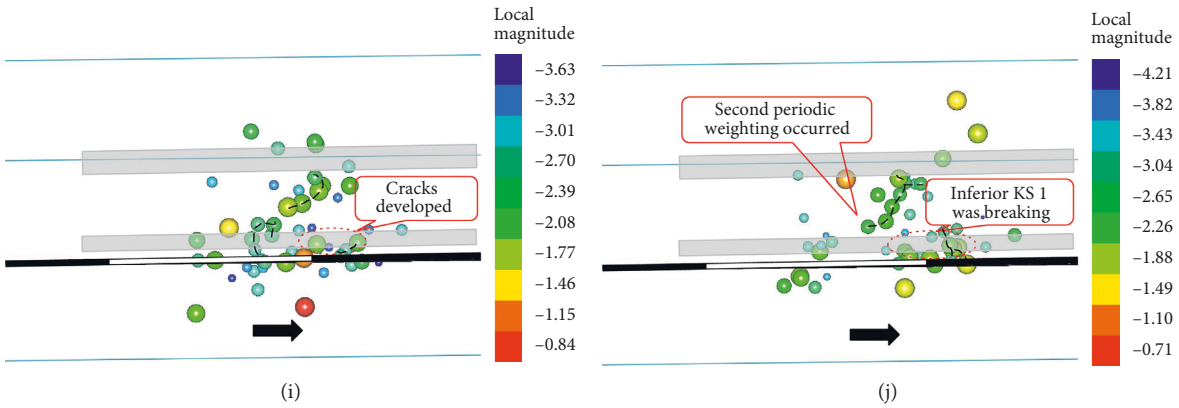

Figure 5: MS events evolution of the inferior KS breakage: (a) Aug 31, (b) Sep 1, (c) Sep 3, (d) Sep 4, (e) Sep 5, (f) Sep 6, (g) Sep 7, (h) Sep 8, (i) Sep 9, and (j) Sep 10.

Several MS events occurred on Aug 31 (Figure 5(a)); yet, there were also few MS events appearing in the inferior KS 1 and 2. It shows that there was no breakage in the two KS at this period, but only a small number of microcracks.

The number of MS events maintained at a lower level on Sep 1 (Figure 5(b)). Few MS events distributed sporadically, and there is still no breakage in the KS. The MS equipment failure caused the lack of MS data on Sep 2.

The number of MS events increased dramatically, and the distribution range was significantly larger than that on Sep 3 (Figure 5(c)). Multiple centralized MS events occurred in inferior KS 1 of the working face. This means that the inferior KS 1 (main roof) is broken and the first weighing occurs, which coincides with the first weighing time described by the stope worker. In the weak strata between inferior KS 1 and 2, MS events are less distributed, and the damage is not serious at this time. Although the main roof is broken, there are not many cracks in the weak strata. Because the weak stratum has not been damaged too much, the whole inferior KS 2 will not be broken. According to the location of MS events, only a small number of MS events are distributed in the inferior KS 2, indicating that only local cracks or cracks occur. Because the length of the working face is 240 m, it is impossible for all parts of KS fracture to keep synchronization. As the weight of the main roof of different parts has a certain time sequence, the weight of the main roof will last for some time.

The number of MS events continued to increase and the range of distribution was further expanded on Sep 4 (Figure 5(d)). There were high concentration of MS events near the main roof, and the weighting of main roof continued. Moreover, there were many MS events in the weak rock strata between the two inferior KS, which indicates that the main roof weighting and breakage caused crack coalescence of the upper rock strata. An area of relatively developed fractures had formed, that is, the fractured zone. And because of the continuous failure of the weak rock strata, there would exist the bed separation below the inferior KS 2. When the bed spacing is large enough, KS will break. From the distribution of MS events, the MS events in inferior KS 2 are clustered in a small range. The results show that it also has some damage, but the damage degree is less than that in the inferior KS 1. Due to the control of inferior KS 2, the upper strata are also broken.

The first weighting was end on Sep 5, and the number of MS events fell quickly (Figure 5(e)). However, because of the continuous mining of the working face, the cracks in the rock strata were also occurring. The MS events in the inferior KS 1 declined suddenly, but the local fissures were still developing caused by bed separation due to the rock strata falling with the mining. The MS events did not gather, indicating that the cracks did not pass through, and the inferior KS 1 did not break. There were also several MS events in the inferior KS 2, with only a small number of cracks being produced.

The large magnitude MS events occurred in the inferior KS 1 on Sep 6 (Figure 5(f)), which shows that it produced large-scale cracks. It may be a precursor to the breakage of KS. The height of MS events was much lower than before, but a few MS events were still distributed in the inferior KS 2, indicating the development of cracks.

The number of MS events rose up on Sep 7 (Figure 5(g)), with a concentration area of MS events running through the inferior KS 1. Then, the main roof broke down and the first periodic weighting of the working face occurred. The collapse of the main roof also destroyed the weak rock strata above the roof. There were some MS events in the inferior KS 2, and cracks or local breakage were also produced.

The number of MS events fell back again (Figure 5(h)), and the first periodic weighting was ended on Sep 8. However, with the continuous excavation of the working face, a small amount of MS events in the inferior KS 1 and 2 indicated that the cracks were beginning to develop continuously.

The number of MS events increased a little on Sep 9 (Figure 5(i)). The MS events in the inferior KS 1 and 2 above the working face were still less distributed, and there were no penetrating cracks formed.

A small range of MS events occurred in the inferior KS 1 on Sep 10 (Figure 5(j)). Cracks in rock mass develop and penetrate, which causes the main roof to rupture again, leading to the second periodic weighting. Although there are

a few MS events in the inferior KS 2, the strata above KS 2 are broken, and some cracks or damages may occur in the inferior KS 2.

According to the analysis of Figure 5, at the first weighting of high-intensity mining working face 11203, two inferior KS all broke down due to the large overhanging area. The periodic weightings were the breakage of the inferior KS 1 and the small range cracks or local breakage of the inferior KS 2, and even only the breakage of the inferior KS 1 and little effect on the inferior KS 2.

4.2.2. Stress and Deformation Evolution of the Inferior KS 1. According to the rock mechanics theory, when the rock is close to the failure state, the increase of deformation accelerates and the increase of stress decreases. After reaching the peak value, the stress decreases with the increase of deformation. According to the theory of rock instability, the faster the stress drop is, the more serious the rock instability is. Therefore, the failure evolution law of KS is analyzed by using stress and deformation characteristics. The stress and displacement data in this paper are calculated based on MS data. The stress is the apparent stress calculated from MS monitoring data, and the formula is shown in equation (6). The apparent stress σ_A [28] is defined as the ratio of the radiated seismic energy E and seismic scalar seismic potency P, expressed as

$$\sigma_A = \frac{E}{P}. \tag{6}$$

The displacement is also calculated based on MS monitoring data. Strain drop method is used to estimate the peak (maximum) displacement at the source in the manuscript. This method directly estimates the peak displacement.

Figure 6 shows the apparent stress and the displacement of the inferior KS 1. Before Sep 3rd, the changes of the apparent stress and the displacement were not large, namely, the rock mass had not been damaged in a large scale. On Sep 3rd, the variation range of the apparent stress increased obviously, and the displacement increased an order of magnitude, indicating that the inferior KS 1 broke down and the first weighting occurred. On Sep 4th, the changes of the apparent stress and the displacement were basically maintained at a level on Sep 3rd, and the first weighting sustained. On Sep 5th, the apparent stress and the displacement decreased, and the first weighting ended. On Sep 7th, the variation range of the apparent stress and the displacement increased again, showing a periodic change, and the first periodic weighting occurred. After that, the change of the apparent stress and the displacement shows a periodic process from decreasing to increasing, but there was a little change in the amount, which indicates that the periodic weightings of the working face were not obvious.

4.2.3. Stress and Deformation Evolution of the Inferior KS 2. Figure 7 shows the apparent stress and the displacement of the inferior KS 2. Before Sep 3rd, the variation of the apparent stress and the displacement were very small, and the inferior KS 2 was almost unaffected. On Sep 3rd, the inferior KS 1 broke down and the first weighting occurred. Then affected by it, the variation range of the apparent stress and the displacement of the inferior KS 2 also increased rapidly, and the local fissures or damage were formed in the inferior KS 2. On Sep 4th, the apparent stress and the displacement increased continuously and the inferior KS 2 broke down. On Sep 5th, the apparent stress and the displacement decreased, and the first weighting ended. On Sep 7th, the first periodic weighting of the working face occurred. The apparent stress and the displacement of the inferior KS 2 increased again, and the rock mass was fractured or damaged. After that, the periodic weightings were not obvious. The apparent stress and the displacement changed little. That is, the inferior KS 2 was not affected by the periodic weightings, and there was no breakage again.

4.2.4. Results of Mine Pressure Monitoring. While the working face was continuously advancing, the resistance monitoring of the hydraulic support was also carried out. The monitoring equipment is shown in Figure 8. There were a total of 142 hydraulic supports in working face 11203, and seven pressure monitoring equipment were installed in which the monitoring data of hydraulic support No. 41 and No. 115 are selected, as shown in Figure 9. The criterion for determining the working face weighting is shown in the following equation [27]:

$$P_{LY} = \overline{P} + \sigma_P. \tag{7}$$

Here, P_{LY} is the working resistance to determine working face weighting, $\overline{P}$ is the average working resistance during the monitoring period, and σ_P is the mean square deviation of working resistance. By comparing the working resistance calculated by equation (7) with that monitored, the weighting of working face can be judged. The calculated working resistances of hydraulic support No. 41 and No. 115 are 38.22 and 30.89 MPa, respectively, and the results are shown in Figure 9. It can be seen that the first weighting occurred on Sep 4th, the first periodic weighting occurred on Sep 7th and 8th, and the second periodic weighting occurred on Sep 10th. However, the location of MS monitoring showed that the first weighting occurred on Sep 3rd and 4th. It may be that on Sep. 3rd, a large number of cracks appeared in the strata, but no large-scale collapse occurred, resulting in a large number of MS events, but there is no abnormal value of hydraulic support pressure. On Sep 4th, the strata collapsed greatly and the pressure of hydraulic support increased sharply. The pressure monitoring results of hydraulic support are basically consistent with those of MS monitoring analysis.

5. MS Parameter Characteristics of the KS Breakage

According to seismological theory, the stability of rock mass is usually determined by statistical analysis based on temporal and spatial evolution of MS events. KS plays an important role in controlling the activities of overlying strata in

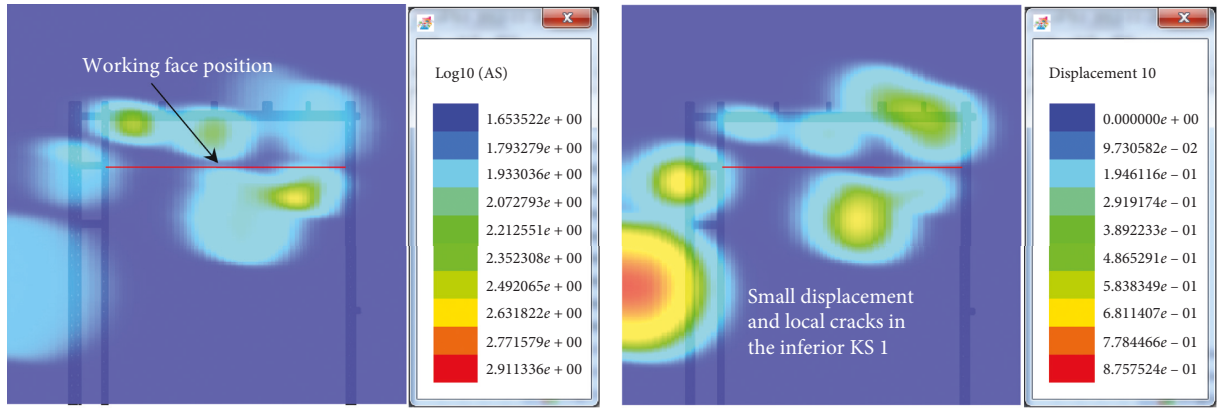

(a)

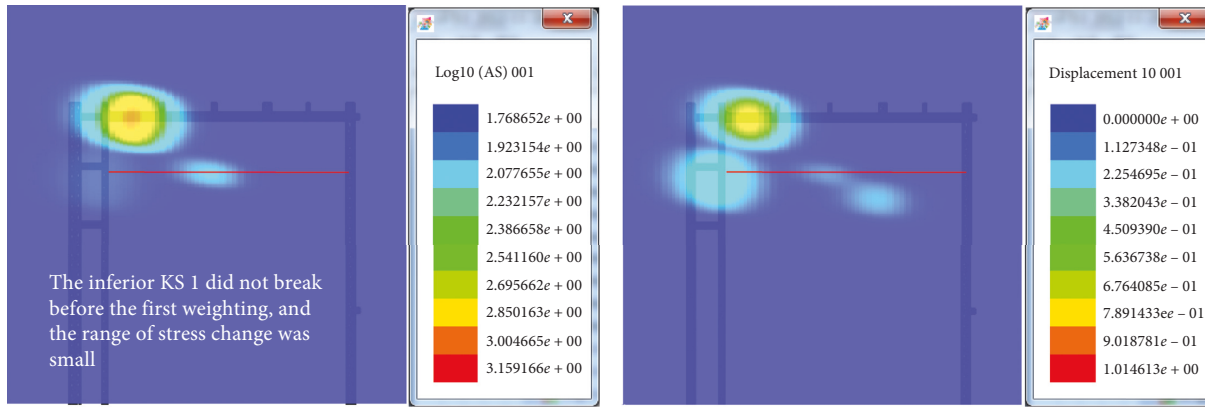

(b)

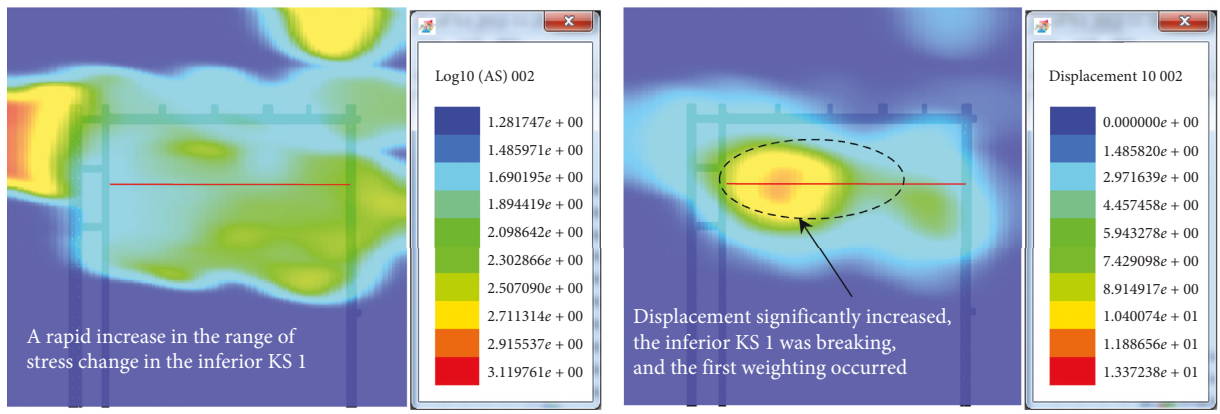

(c)

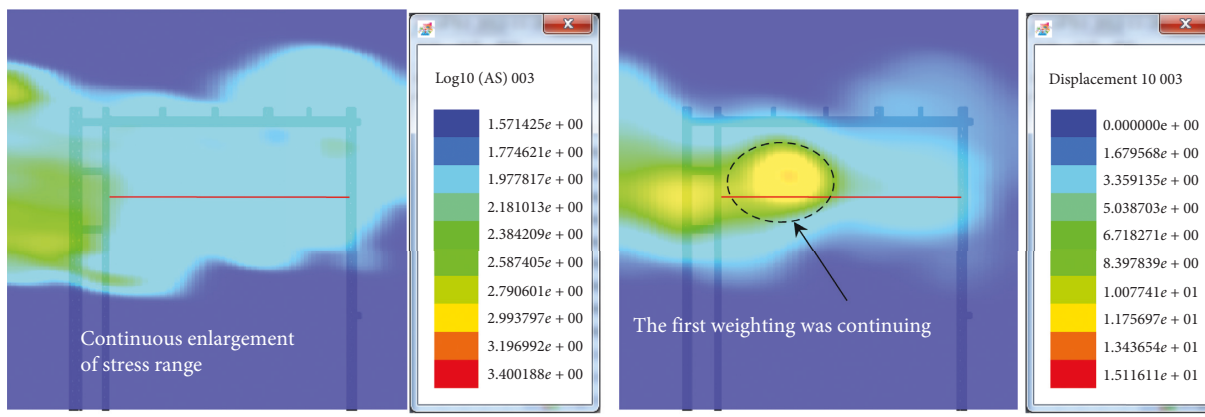

(d)

Figure 6: Continued.

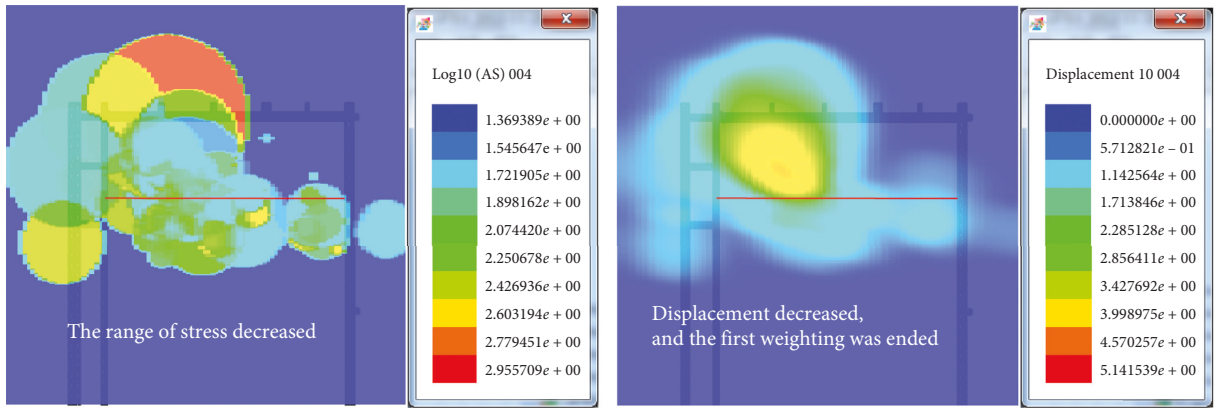

(e)

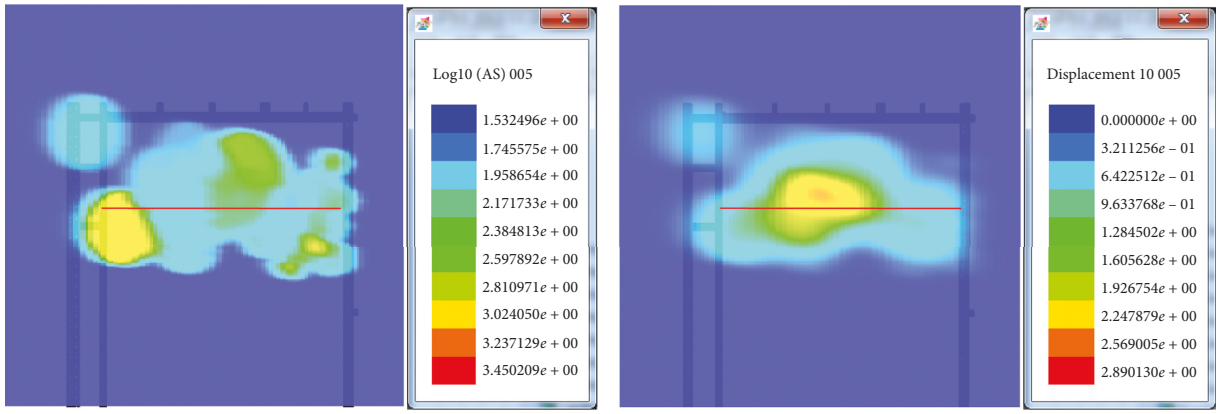

(f)

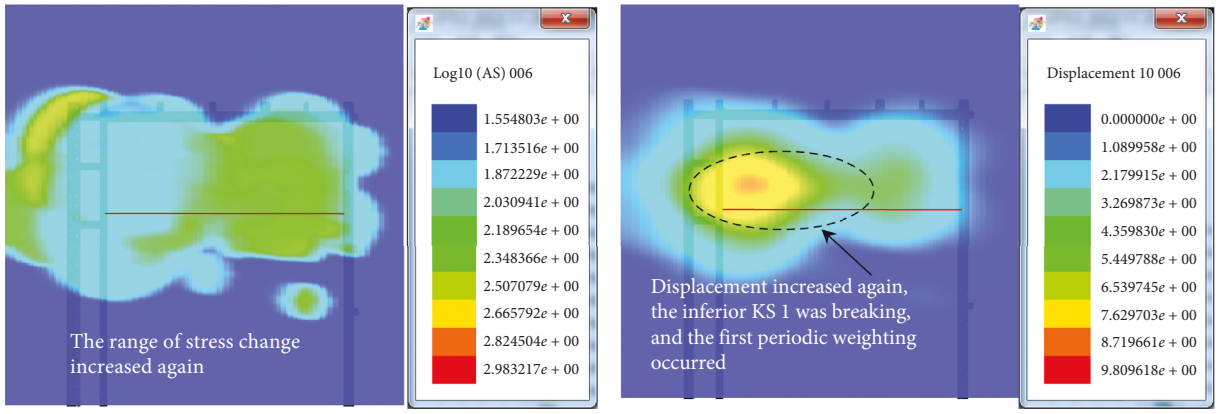

(g)

Figure 6: Continued.

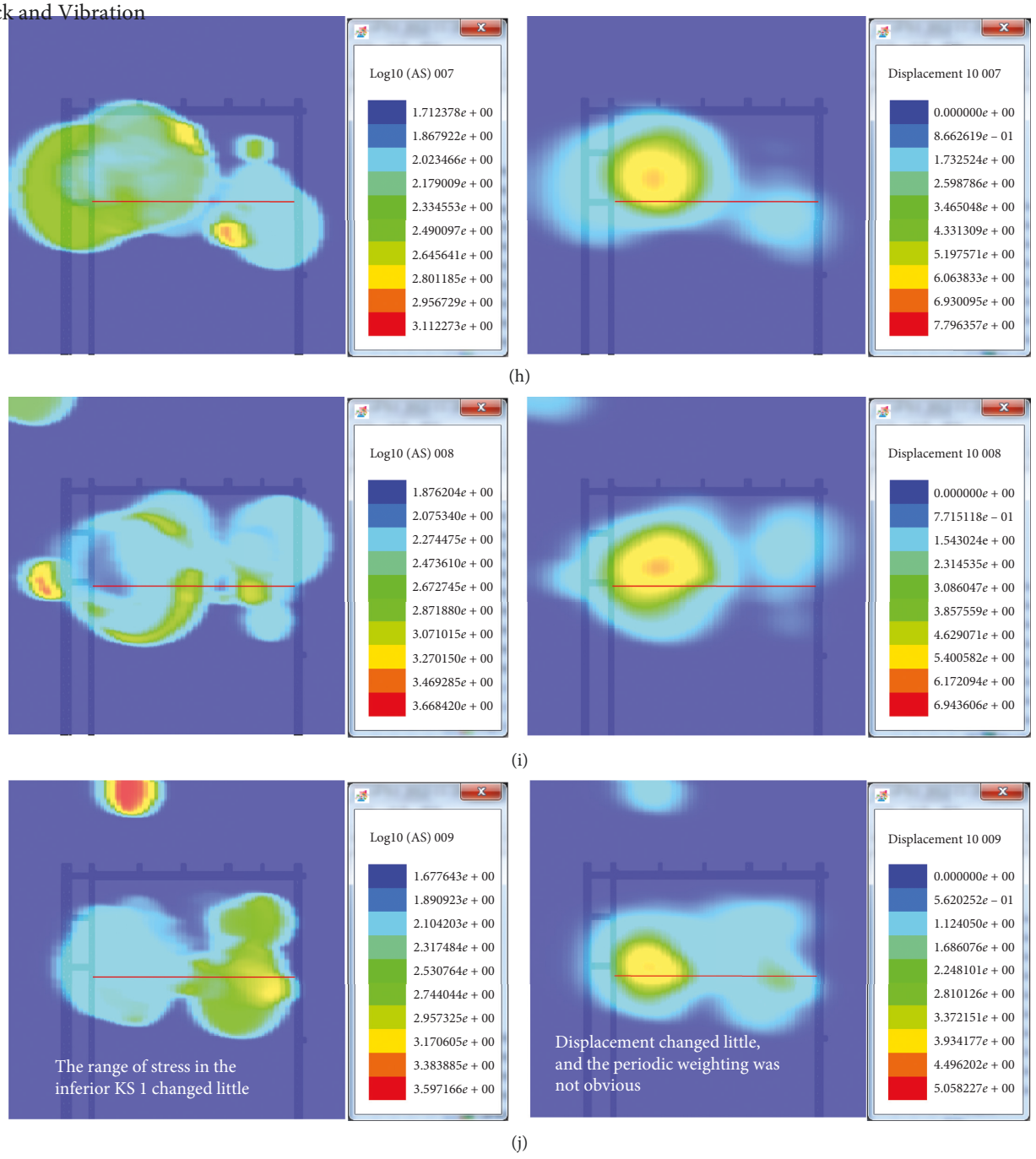

Figure 6: Cloud charts of apparent stress and displacement in inferior KS 1: (a) Aug 31, (b) Sep 1, (c) Sep 3, (d) Sep 4, (e) Sep 5, (f) Sep 6, (g) Sep 7, (h) Sep 8, (i) Sep 9, and (j) Sep 10.

stope. Therefore, the KS breakage has an important impact on the pressure characteristics of the mine. It may lead to mine dynamic phenomena and then lead to serious geological disasters. Therefore, the evolution characteristics of the event number, energy release, energy index, Schmidt number, coefficient of seismic response, and b value and their relationship with KS breakage are studied.

Selecting the MS data from Aug 20 to Sep 11, 2013, the characteristics of MS parameters are analyzed. Among them, the first weighting occurs on Sep 3rd and 4th, as shown in Figure 5. The first periodic weighting occurred on Sep 7th, and the second periodic weighting occurred on Sep 10th. Taking three weights as an example, the stability of KS is judged by the characteristics of MS parameters when roof weighting (KS breaking) occurs under high-intensity mining conditions.

5.1. MS Event Number. Mining coal from the working face will cause fracture and damage of the surrounding rock, accompanied by a large number of MS events in this process. MS event number is a MS parameter which can reflect the degree of the surrounding rock failure to a certain extent.

Figure 10 shows the changes of MS event number with time. At the three weightings, MS event number increased sharply. But at the other time, MS event number was low. It

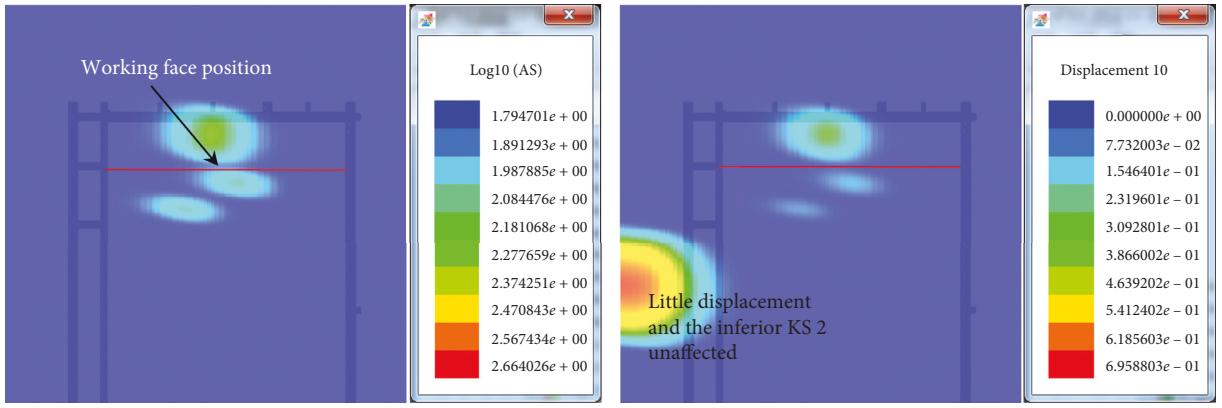

(a)

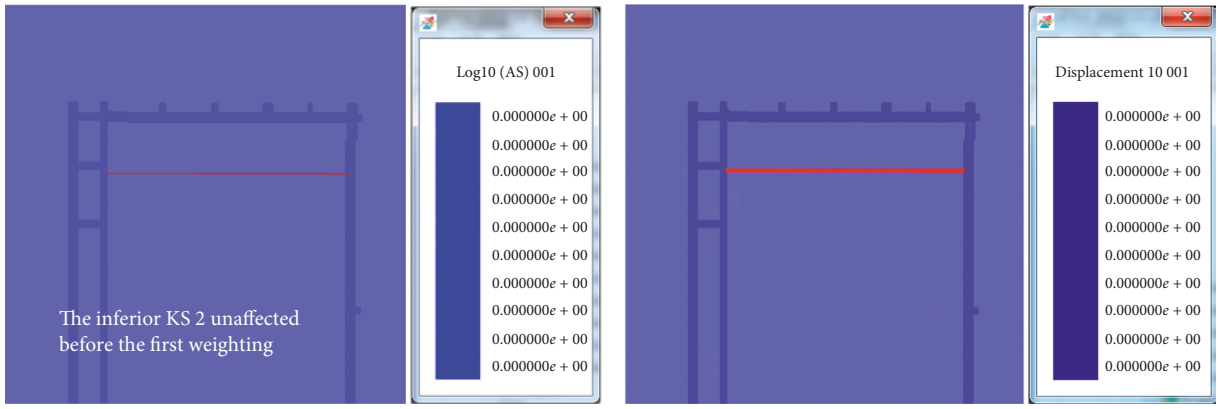

(b)

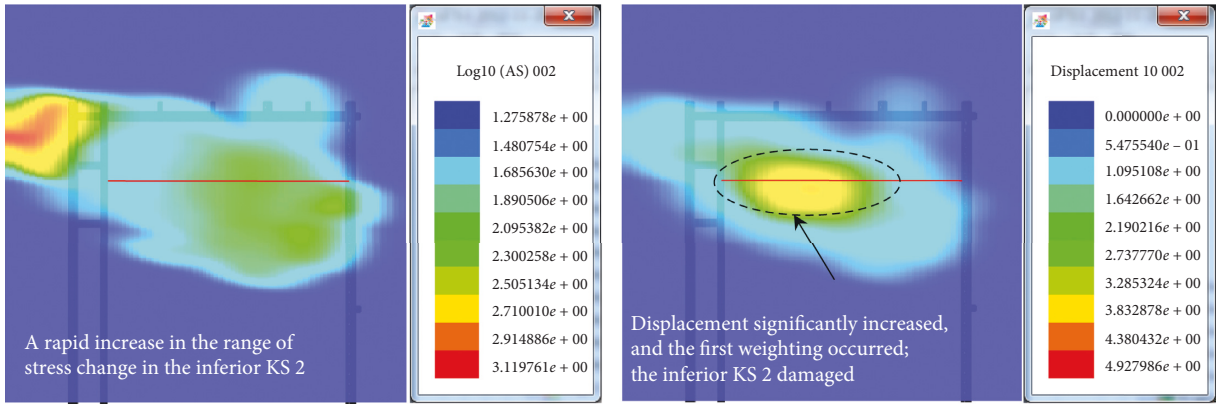

(c)

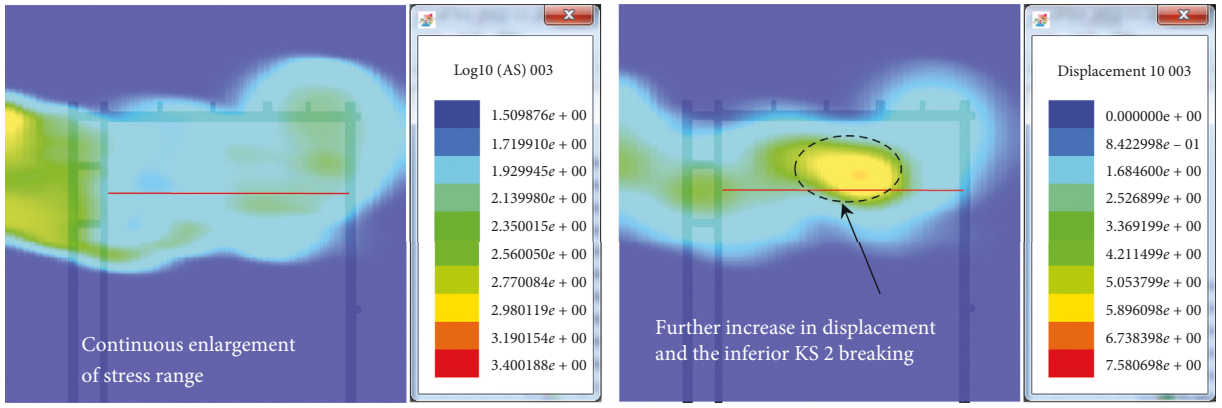

(d)

Figure 7: Continued.

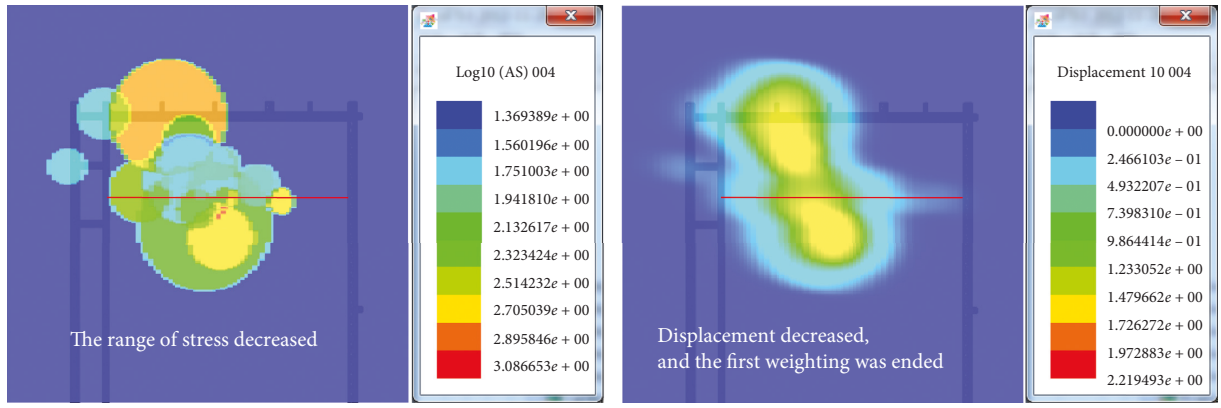

(e)

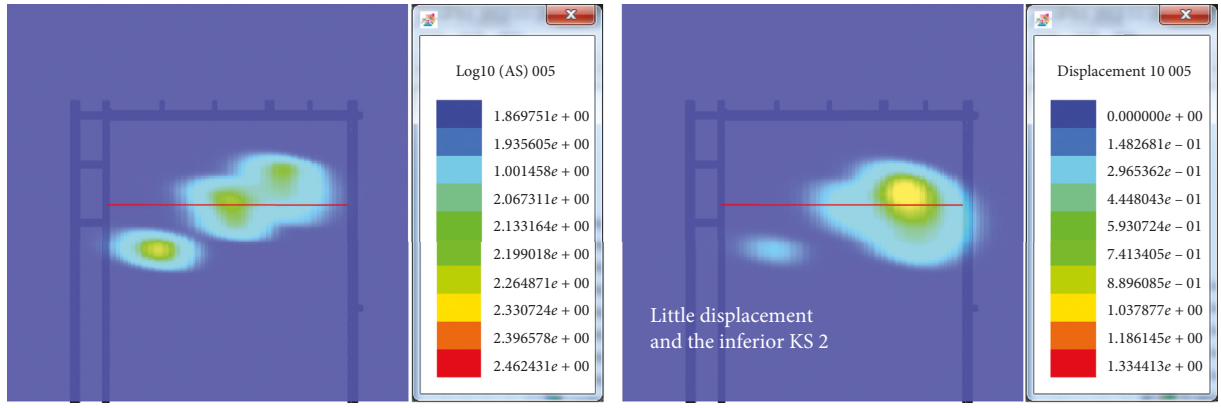

(f)

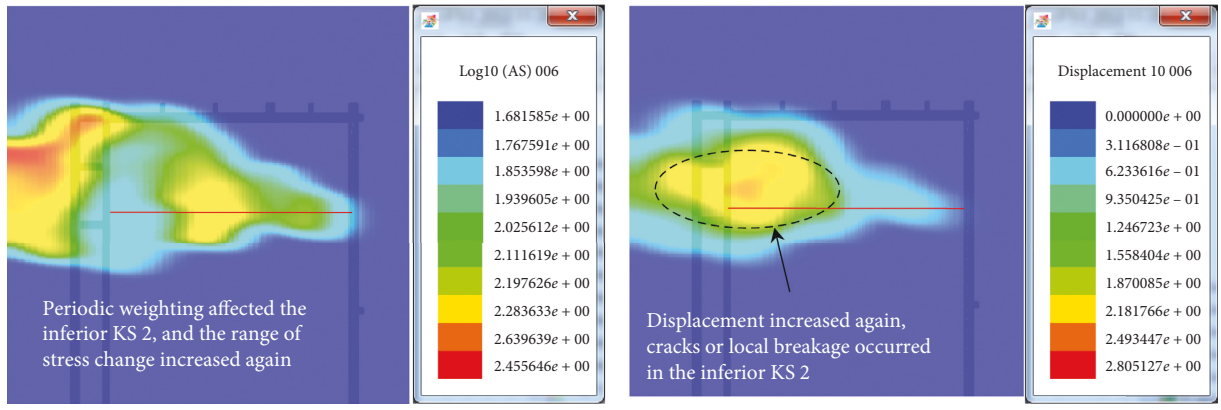

(g)

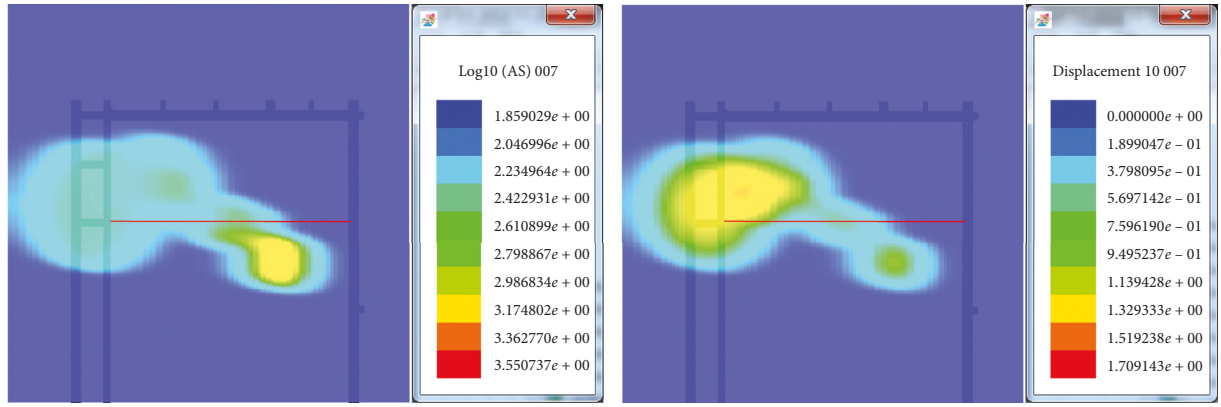

(h)

Figure 7: Continued.

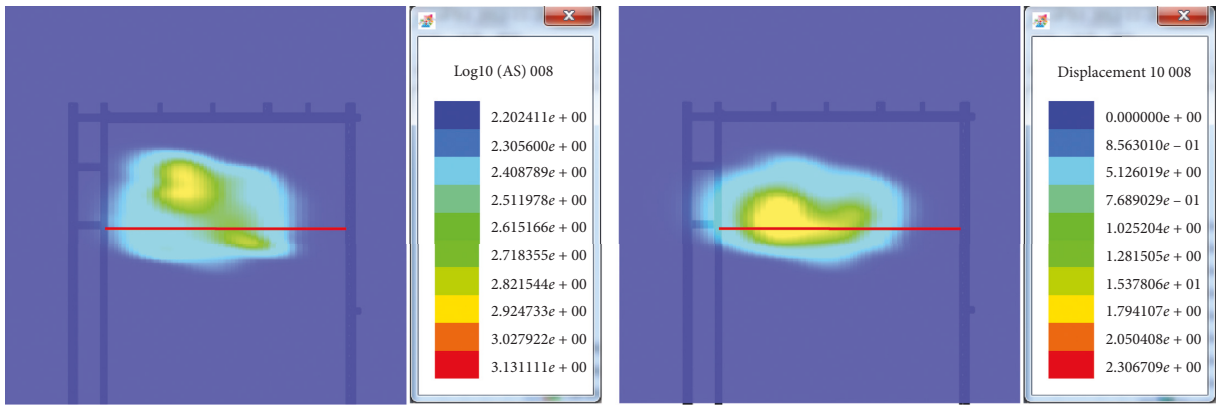

Figure 7: Cloud charts of apparent stress and displacement in inferior KS 2. (a) Aug 31, (b) Sep 1, (c) Sep 3, (d) Sep 4, (e) Sep 5, (f) Sep 6, (g) Sep 7, (h) Sep 8, (i) Sep 9, and (j) Sep 10.

(a) (b)

Figure 8: Pressure monitoring of hydraulic support in the working face. (a) Hydraulic support in the working face and (b) pressure monitoring equipment.

reflects that the roof weighting has a good correspondence with the MS event number.

5.2. Energy Release. The energy release of MS events can also reflect the damage degree of the surrounding rock. Figure 11 shows the variation of energy release over time. At the first weighting, it is clear that the energy release increases significantly and reaches its maximum. The energy release increases slightly with periodic weighting. Because the periodic weighting intensity is less than the first weighting, the energy release is also smaller. Similar to the number of MS events, energy release also has a good relationship with roof weighting.

5.3. Energy Index. Energy index (EI) [28] of a MS event is the ratio of the observed radiated seismic energy of that event E to the average energy $\overline{E}(P)$ radiated by events of the observed potency P taken from $\log \overline{E}(P) = d \log P + c$, where

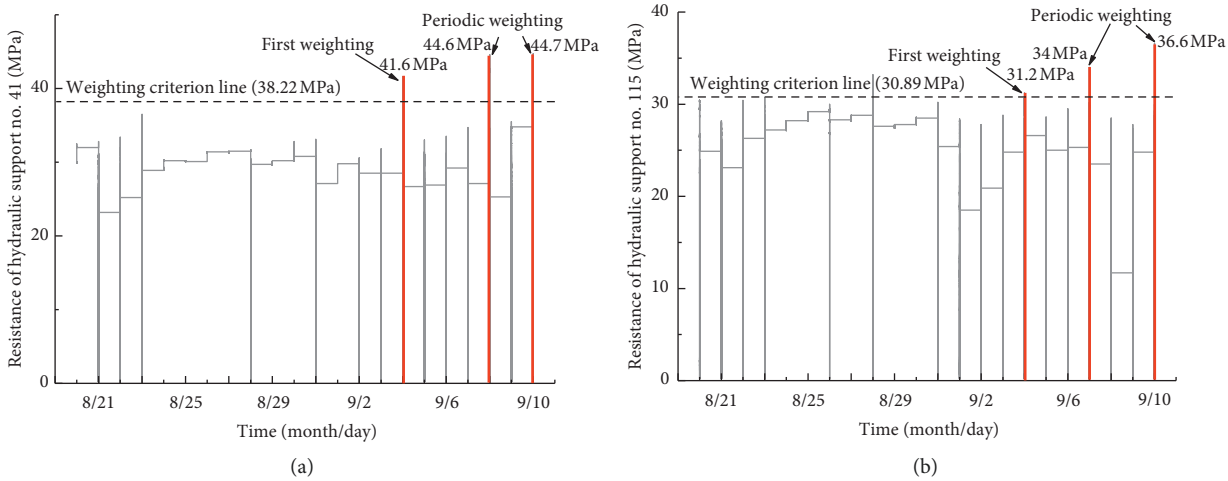

Figure 9: Working resistance of the hydraulic support in the working face. Resistance of (a) hydraulic support no. 41 and (b) hydraulic support no. 115.

$d = 1.0$ would be proportional to the apparent stress. The higher the energy index, the higher the driving stress at the source of the event when it occurs. Therefore, the changes of energy index (EI) can be applied to obtain precursor information of rock mass hazards:

$$\mathrm{EI}(P) = \frac{E}{\overline{E}(P)} = \frac{E}{10^{d \log P + c}} = 10^{-c} \cdot \frac{E}{P^d}. \tag{8}$$

The changes of energy index are shown in Figure 12. Before the first weighting and the periodic weighting, energy index had a sudden drop, demonstrating the release of the stress of surrounding rock, with the KS being close to break.

5.4. Schmidt Number. Schmidt number, Sc, [28] can measure the spatiotemporal complexity of seismic flow of rock and is the only parameter reflecting the potential instability. The lower the Schmidt number is, the more unstable the MS deformation will be. In the analysis of general logarithm, the cumulative volume combination can effectively judge the stability of rock mass. We often use its logarithmic form, combined with cumulative apparent volume, to analyze stability of rock mass. MS information for Schmidt number include time t, location $X(x, y, z)$, seismic moment M and its tensor M_{ij}, and radiated energy E, which can be obtained from the MS waveform.

Schmidt number is defined as

$$\mathrm{Sc}(\Delta V \Delta t) = \frac{4\Delta V \Delta t(\overline{t}) \sum_{t_1}^{t_2} E}{\rho(\overline{X})^2 \left(\sum_{t_1}^{t_2} M_{ij}\right)}, \tag{9}$$

where MS events occurred in the volume ΔV and the time Δt, $\Delta t = t_2 - t_1$, $\overline{X}$ is an average distance between consecutive sources of interacting seismic events, ρ is the rock density, and $\overline{t}$ is an average time between events. Schmidt number encompasses four independent parameters which describe seismicity, namely, $\overline{t}$, $\overline{X}$, $\sum E$, and $\sum M_{ij}$.

The changes of Schmidt number are shown in Figure 13. Similar to energy index, Schmidt number fell suddenly before the weightings and had some precursory characteristics.

5.5. Coefficient of Seismic Response. In the analysis of MS events caused by mining activities, the specific mining information (e.g., ore mining volume) should be closely combined to obtain more accurate and practical results. Therefore, it is necessary to find a physical quantity to characterize the relationship between energy storage and release in the process of mining, so as to reflect the response characteristics of MS activities. Coefficient of seismic response (CSR) proposed by Tang et al. [29] is a physical quantity reflecting these characteristics.

CSR is defined as

$$\mathrm{CSR} = \frac{\sum V_{\mathrm{A}}}{\sum V_m}. \tag{10}$$

According to the definition of CSR, the change of CSR reflects the sensitivity of mining MS activity, namely, the response speed and response intensity. With the increasing of CSR, a small amount of mining will cause large MS activities, and vice versa. Therefore, CSR can be used to evaluate the stability tendency of the mine rock mass system. Figure 14 shows the changes of CSR. At the first weighting, CSR rose rapidly, indicating that KS shows the higher instability level. At the periodic weighting, CSR increased more slowly than the first weighting, so the stability of KS was better than the first weighting, because the strength of the first weighting was greater than the periodic weighting.

5.6. b Value. Many observations show that MS events induced by mining have the same regularity as natural earthquakes. The magnitude-frequency relationship proposed by Gutenberg and Richter [30] is followed in the analysis of these two types of seismicity:

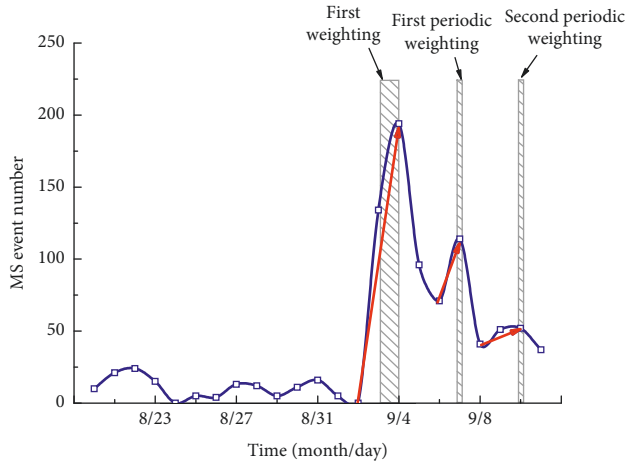

Figure 10: Changes of the MS event number with time.

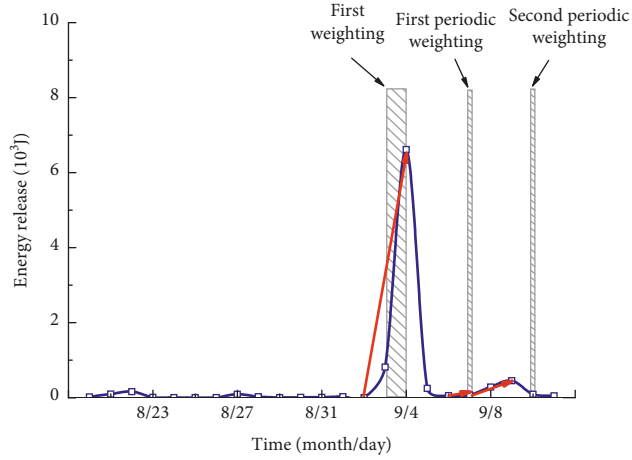

Figure 11: Changes of energy release with time.

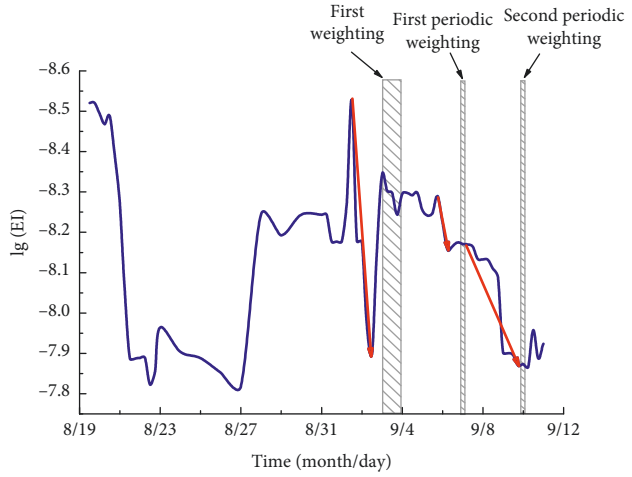

Figure 12: Changes of energy index with time.

$$\lg N = a - bM, \tag{11}$$

where M is the magnitude, N is the number of earthquakes with magnitude equal or above M, a and b are constants, and

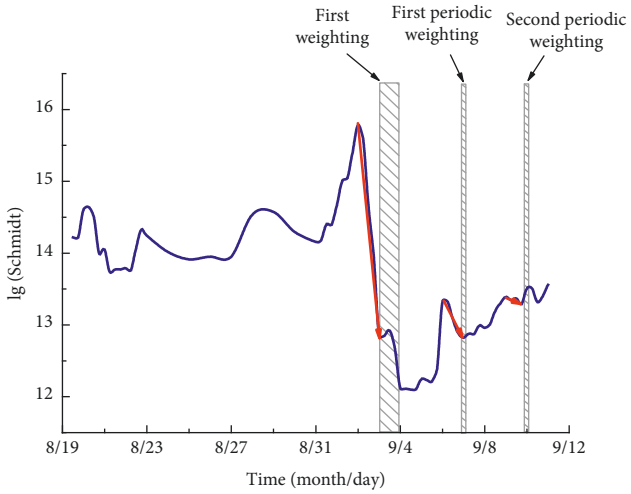

Figure 13: Changes of Schmidt number with time.

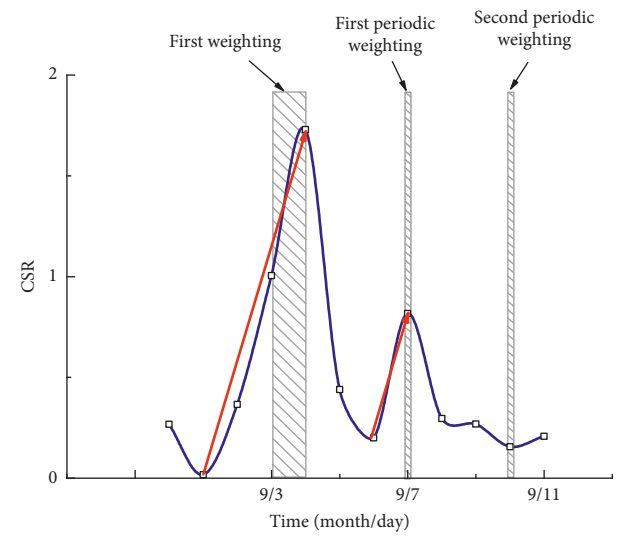

Figure 14: Changes of CSR with time.

b value is the function of magnitude distribution and crack extension scale. Rock stress state is closely related to b value. The continuing decline of b value indicates the increase of large-scale cracks and differential stress in rock mass. b value is not only a statistical analysis parameter, but has direct physical meaning.

In this paper, the least squares method was used to calculate b value, with magnitude interval $\Delta M = 0.275$ also being adopted. Using the sliding window to calculate b value, 100 MS events and 50 MS events were adopted as calculated window and sliding window, respectively. The changes of b value are shown in Figure 15. Before the three weighting, b value declined rapidly, indicating that large-scale failure was increasing and the KS was in an unstable state.

6. Discriminant Method of the KS Breakage

It is limited to judge the breakage of KS from a single MS parameter, so it is difficult to accurately predict and judge the

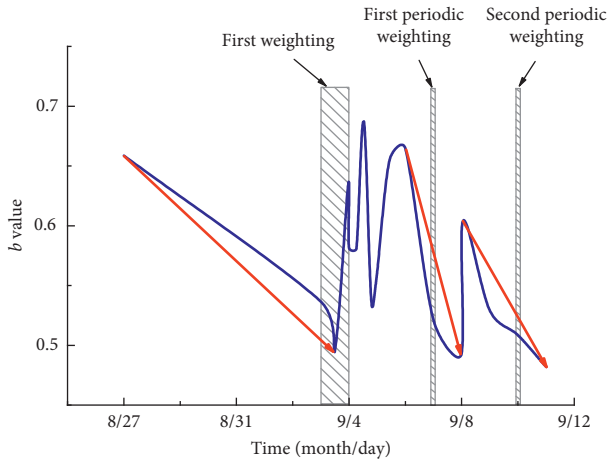

Figure 15: Changes of b value with time.

failure of KS. However, by synthetically judging the characteristics of multiple MS parameters, the breakage of KS can be determined more comprehensively and scientifically. According to the characteristics of MS parameters, the prediction period (sudden rise or decline) of MS parameters before the first weighting and periodic weighting can be obtained.

Figure 16 shows the predictive periods of MS parameters. Each MS parameter of the predictive period was not same, and the predictive order of the same MS parameter at different weightings was also different. But taking the first weighting as an example, it is not difficult to find only a few parameters appeared in the forewarning characteristics before a long period of the weighting, but near to the weighting time, almost all parameters appeared anomaly. Therefore, we can judge the stability of KS according to the number of abnormal MS parameters. Here, the forewarning levels are introduced to divide the four stability grades of KS. Grades one, two, three, and four are expressed as red, yellow, orange, and blue warning, respectively, and grade one is the highest level. That is, the red warning indicates that the KS is the most unstable, while the blue warning indicates that the KS is stable. If only one MS parameter appears the forewarning characteristic, it is considered as blue warning period, showing the good stability of KS. If two MS parameters appear the forewarning characteristic, it is considered as yellow warning period, showing the general stability of KS. If three or four MS parameters appear in the forewarning characteristic, it is considered as orange warning period, showing the bad stability of KS. If five or six MS parameters appear in the forewarning characteristic, it is considered as red warning period, showing the very bad stability of KS. When almost all MS parameters appeared anomaly (in red warning period), the KS would break, which can be taken as the criterion of the breakage of KS. The method to discriminate the stability of KS is shown in Figure 17.

We define $N(t)$, $E(t)$, EI (t), Sc (t), CSR (t), and $b(t)$ as the time-varying functions of event number, energy release, energy index, Schmidt number, CSR, and b value, respectively. From the changes of event number in Figure 16, it

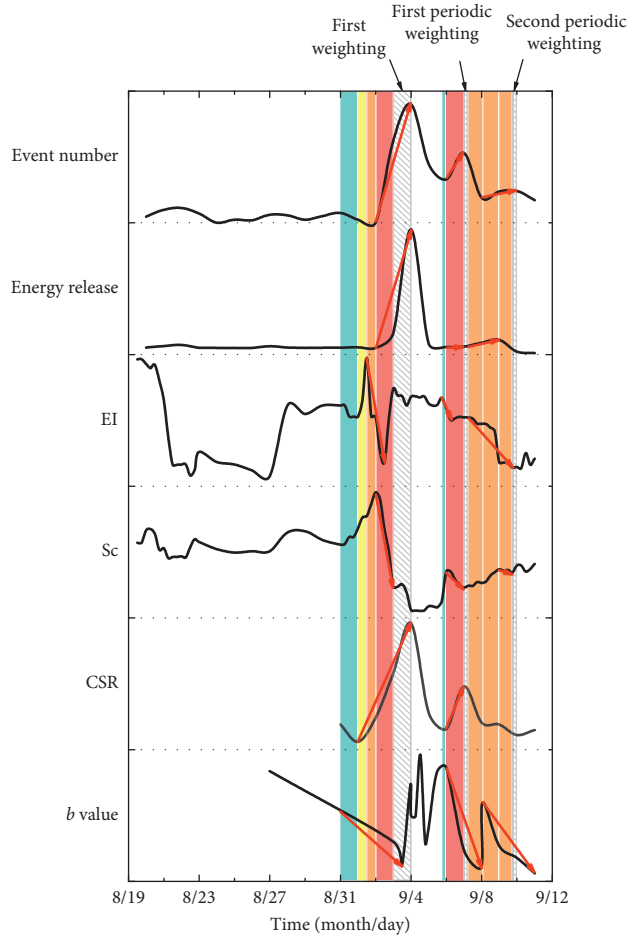

Figure 16: Warning time of MS parameters.

can be seen that the event number increased before the breakage of KS, so the slope of tangent to the curve $N(t)$ was greater than zero, namely, $N'(t) > 0$. Similarly, according to the changes of each MS parameter characteristics, equation (12) can be obtained.

$$\begin{cases} N'(t) > 0, \\ E'(t) > 0, \\ \mathrm{EI}'(t) < 0, \\ \mathrm{Sc}'(t) < 0, \\ \mathrm{CSR}'(t) > 0, \\ b'(t) < 0. \end{cases} \tag{12}$$

The breakage of KS needs to meet equation (12), which can be used to discriminate the breakage of KS based on MS parameters. Through combining the locations of MS events, the specific location of rock failure can be specified.

The rock fracture range caused by coal mining is 80 m, and the KS which controls these rock strata is the inferior KS 2. Therefore, in this paper, the KS judged whether breaking or not is the inferior KS 2. Then, we can use this method to judge the breaking of the inferior KS 2 of the two periodic weightings. There was only a short blue warning period

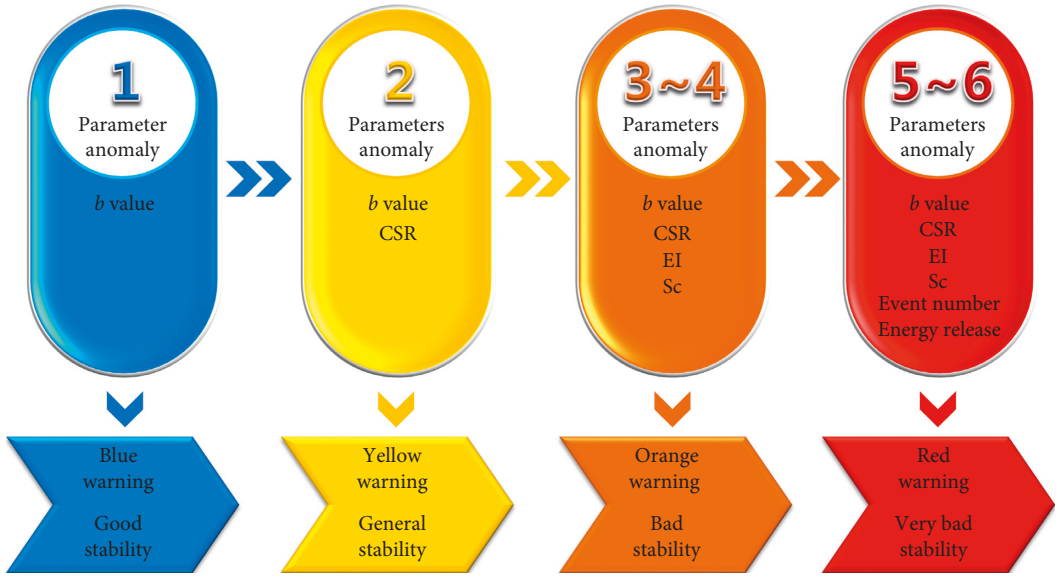

Figure 17: Method to discriminate the stability of KS.

before the first periodic weighting, and then all MS parameters appear abnormal and enter the red warning period, that is, the inferior KS 2 will break. But before the second periodic weighting, there was only an orange warning period and no red warning period. Because the weighting intensity is not very high, the inferior KS 2 will not fracture completely. Not all four warning periods will appear in every judgment. Other periodic weightings can also be similar to judging the stability of the inferior KS 2, which is mentioned in detail here. This method can not only predict the stability of KS but also forewarn geological hazards. It can provide guidance for disaster prevention and control of high-intensity mining working face by combining the location of MS events and the value of MS parameters.

7. Conclusions

The KS plays a controlling role in the movement of the rock strata. MS monitoring was carried out in working face 11203 of the Xiaojihan coal mine, and the evolution law of MS events and the characteristics of MS parameters were also analyzed. The main conclusions are as follows.

There are a main KS and four inferior KS in the working face 11203, according to the discriminant method of the KS breakage. The pressure behavior of the working face is affected by the inferior KS 1 and 2. With the high-intensity mining of the working face 11203, the inferior KS 1 and 2 were breaking when the first weighting occurred. The periodic weightings were the breakage of the inferior KS 1 and the small range cracks or local breakage of the inferior KS 2.

Before the breakage of KS, there were forewarning characteristics (sudden rise or decline) in MS event number, energy release, energy index, Schmidt number, CSR, and b value. According the forewarning characteristics and the forewarning levels, this paper proposed the method to discriminate the breakage of KS. Based on the MS monitoring, MS parameters appearing anomaly can be taken as the criterion of the breakage of KS, thereby providing a new attempt to study the breakage of KS.

Data Availability

The data used to support the findings of this study are available from the corresponding author upon request.

Conflicts of Interest

The authors declare that there are no conflicts of interest regarding the publication of this paper.

Acknowledgments

The authors are grateful to the China University of Mining and Technology for the pressure data support of working face 11203 of the Xiaojihan coal mine. The authors gratefully acknowledge the support from the China Postdoctoral Science Foundation (2018M641200), Fundamental Research Funds for the Central Universities (FRF-TP-18-021A1), National Program on Key Basic Research Project (973) Program (2013CB227902), and National Key R&D Program of China (2017YFC0602901).

References

[1] H. Ding, X. Miao, F. Ju, X. Wang, and Q. Wang, "Strata behavior investigation for high-intensity mining in the water-rich coal seam," *International Journal of Mining Science and Technology*, vol. 24, no. 3, pp. 299–304, 2014.

[2] Research Group of National Key Basic Research Program of China, "Theory and method research of geological disaster prevention on high-intensity coal exloitation in the West areas," *Journal of China Coal Society*, vol. 42, no. 2, pp. 267–275, 2017.

[3] X. X. Miao, Protection introduction of basic research on geological disaster prevention and environmental of western coal under high mining intensity, 2016.

[4] L. M. Fan, X. D. Ma, H. Jiang, and C. Shuai, "Risk evaluation on water and sand inrush in ecologically fragile coal mine," *Journal of China Coal Society*, vol. 41, no. 3, pp. 531–536, 2016.

[5] G. Zhang, K. Zhang, L. Wang, and Y. Wu, "Mechanism of water inrush and quicksand movement induced by a borehole and measures for prevention and remediation," *Bulletin of Engineering Geology and the Environment*, vol. 74, no. 4, pp. 1395–1405, 2015.

[6] M. G. Qian, X. X. Miao, and J. L. Xu, "Theoretical study of key stratum in ground control," *Journal of China Coal Society*, vol. 21, no. 3, pp. 225–230, 1996.

[7] X. X. Miao and M. G. Qian, "Broken feature of key strata and its influence on rock pressure in super-length fully-mechanized coal face," *Chinese Journal of Rock Mechanics and Engineering*, vol. 22, no. 1, pp. 45–47, 2003.

[8] X. X. Miao, R. H. Chen, H. Pu et al., "Analysis of breakage and collapse of thick key strata around coal face," *Chinese Journal of Rock Mechanics and Engineering*, vol. 24, no. 8, pp. 1289–1295, 2005.

[9] S. J. Gibowicz and A. Kijko, *An Introduction to Mining Seismology*, Academic Press, Cambridge, MA, USA, 1994.

[10] M. Cai, P. K. Kaiser, and C. D. Martin, "Quantification of rock mass damage in underground excavations from microseismic event monitoring," *International Journal of Rock Mechanics and Mining Sciences*, vol. 38, no. 8, pp. 1135–1145, 2001.

[11] R. P. Young and D. S. Collins, "Seismic studies of rock fracture at the underground research laboratory, Canada," *International Journal of Rock Mechanics and Mining Sciences*, vol. 38, no. 6, pp. 787–799, 2001.

[12] M. C. Ge, "Efficient mine microseismic monitoring," *International Journal of Coal Geology*, vol. 64, no. 1-2, pp. 44–56, 2005.

[13] S. L. Li, X. G. Yin, W. D. Zheng et al., "Research of multi-channel microseismic monitoring system and its application to Fankou lead-zinc mine," *Chinese Journal of Rock Mechanics and Engineering*, vol. 24, no. 12, pp. 2048–2053, 2005.

[14] N. W. Xu, F. Dai, Z. Z. Liang, Z. Zhou, C. Sha, and C. A. Tang, "The dynamic evaluation of rock slope stability considering the effects of microseismic damage," *Rock Mechanics and Rock Engineering*, vol. 47, no. 2, pp. 621–642, 2014.

[15] B.-R. Chen, X.-T. Feng, Q.-P. Li, R.-Z. Luo, and S. Li, "Rock burst intensity classification based on the radiated energy with damage intensity at jinping II hydropower station, China," *Rock Mechanics and Rock Engineering*, vol. 48, no. 1, pp. 289–303, 2013.

[16] C.-P. Lu, G.-J. Liu, Y. Liu, N. Zhang, J.-H. Xue, and L. Zhang, "Microseismic multi-parameter characteristics of rockburst hazard induced by hard roof fall and high stress concentration," *International Journal of Rock Mechanics and Mining Sciences*, vol. 76, no. 6, pp. 18–32, 2015.

[17] Y. H. Cheng, F. X. Jiang, J. L. Cheng et al., "The primary study on microseismic locating and monitoring technology of shock bump caused by key stratum movement," *Journal of China Coal Society*, vol. 31, no. 3, pp. 273–277, 2006.

[18] L. M. Dou and H. He, "Study of OX-F-T spatial structure evolution of overlying strata in coal mines," *Chinese Journal of Rock Mechanics and Engineering*, vol. 31, no. 3, pp. 453–460, 2012.

[19] H. He, L. M. Dou, S. Y. Gong et al., "Rock burst rules induced by cracking of overlying key stratum," *Chinese Journal of Geotechnical Engineering*, vol. 32, no. 8, pp. 1260–1265, 2010.

[20] X. F. Xu, L. M. Dou, A. Y. Cao et al., "Effect of overlying strata structures on rock burst and microseismic monitoring analysis," *Journal of Mining and Safety Engineering*, vol. 28, no. 1, pp. 49–51, 2011.

[21] A. Y. Cao, L. L. Zhu, F. C. Li et al., "Characteristics of *T*-type overburden structure and tremor activity in isolated face mining under thick-hard strata," *Journal of China Coal Society*, vol. 39, no. 2, pp. 328–335, 2014.

[22] D. Wei, H. He, Y. F. Qin et al., "Study on mechanism of mining tremor induced by key strata instability in the gob beside the working face," *Journal of China Coal Society*, vol. 35, no. 12, pp. 1957–1962, 2010.

[23] J. Q. Jiang, P. P. Zhang, G. P. Qin et al., "Fracture laws of one-side mined high-position hard thick key strata and microseismic energy distribution," *Journal of Mining and Safety Engineering*, vol. 32, no. 4, pp. 523–529, 2015.

[24] J. Q. Jiang, P. P. Zhang, G. P. Qin et al., "Analysis of destabilized fracture and microseismic activity of high-located main key strata," *Rock and Soil Mechanics*, vol. 36, no. 12, pp. 3567–3575, 2015.

[25] Y. Li, T.-H. Yang, H.-L. Liu et al., "Real-time microseismic monitoring and its characteristic analysis in working face with high-intensity mining," *Journal of Applied Geophysics*, vol. 132, pp. 152–163, 2016.

[26] M. G. Qian, X. X. Miao, J. L. Xu et al., *Key Strata Theory in Ground Control*, China University of Mining and Technology Press, Xuzhou, China, 2003.

[27] M. G. Qian, P. W. Shi, and J. L. Xu, *Mine Pressure and Rock Strata Control*, China University of Mining and Technology Press, Xuzhou, China, 2010.

[28] A. Mendecki, *Seismic Monitoring in Mines*, Chapman & Hall, London, UK, 1997.

[29] L. Z. Tang, J. Zhang, X. B. Li et al., "Research on response of mine microseismicity to mining rate based on quantitative seismology," *Chinese Journal of Rock Mechanics and Engineering*, vol. 31, no. 7, pp. 1349–1354, 2012.

[30] B. Gutenberg and C. F. Richter, "Frequency of earthquakes in California," *Bulletin of the Seismological Society of America*, vol. 34, no. 4, pp. 185–188, 1944.